Toward a Metal-Free Contact Based on Multilayer Epitaxial Graphene on 4H-SiC

Isodiana Crupi, *Senior Member, IEEE*, Gabriele Bellocchi, Roberto Vabres, Corrado Bongiorno, Paolo Badalà, Roberto Macaluso, *Member, IEEE*, Mauro Mosca, and Simone Rascunà

***Abstract*— We report on a promising approach to realize bifacial silicon carbide (SiC) based ultraviolet (UV) photodetectors with no metallic electrodes. The ohmic contact regions, consisting of a few conductive carbon-rich layers, while maintaining the necessary UV sensitivity for the photodetector's operation, are directly realized using a nanosecond-pulsed excimer laser. By combining structural, optical, and electrical characterization, we demonstrate how this treatment allows the formation of ohmic contacts, on both front and rear side, using fluence higher than 1.6 J/cm^2 and 3.2 J/cm^2, respectively.**

***Index Terms*— Excimer laser annealing, multilayer epitaxial graphene, ohmic contacts, silicon carbide.**

I. Introduction

SEMICONDUCTOR materials with wide bandgap, high breakdown field, operating temperature, switching frequencies, thermal conductivity and stability are well-suited for applications in photodetection devices [1]. Silicon Carbide (SiC) has these outstanding physical properties and the photodiodes based on it have excellent performance in harsh environments [2], [3], [4], being suitable for optoelectronic applications in extreme conditions, under high-intensity UV radiation and at high temperature, with sensitivity, response and performance that can be tailored through the appropriate choice of the SiC polytype cubically (3C-SiC) [1], [6], [7] and hexagonally (4H-SiC or 6H-SiC) [8], [9], [10], [11]. Although significant achievements have been made in both SiC material growth and photodetector fabrication, there are still ongoing challenges that need to be addressed [12]. Among them, the careful design and optimization of ohmic contacts are essential for maximizing the performance [13], [14] and translucency of SiC photodetection devices. Well-engineered ohmic contacts in photodetection devices must enable improved transport and collection of charge carriers without affecting the light transmission through the SiC structure. SiC's transparency across a broad frequency range is a key advantage, enabling its photodetectors to effectively detect light. However, the presence of conventional metallic contacts reduces the transparency. Furthermore, the key requirements of an ohmic contact include the need for a flat surface, minimal contact resistivity, and stability. Typically, on the rear side of a SiC device, such as Junction Barrier Schoktty diode (JBS), the ohmic contact is established by depositing a nickel layer, followed by a thermal annealing, whereas on the front side Schottky contacts are established through lithographic processes typically in the comb-fingered form. This geometry is chosen to allow direct exposure to the incident radiation while simultaneously enabling vertical electrical conduction. At present, many studies have been conducted on the performance of the most widely used electrode materials, namely Ni and Ti, on SiC [15], [16], [17], [18]. However, the useful area of the device, that is effectively exposed to the UV radiation, is limited by the presence of these contacts, which strongly absorb the UV radiation. Thus, new solutions must be explored to establish ohmic contacts able to overcome the drawbacks of the comb-finger structure [19]. In this letter, we want to take advantage of the transformation of SiC, at its surface, into a stable ohmic-contact after pulsed laser annealing (PLA) treatment [20], not only on the implanted [21], [22] but also on the unimplanted regions. These contact layers have, for their own nature, the same shape and extension as the irradiated regions and do not extend beyond the surface. Our investigation aims to maximize the active area of a photodetector, setting the stage for future advancements in UV detection technology.

Manuscript received 27 April 2024; revised 14 May 2024; accepted 17 May 2024. Date of publication 21 May 2024; date of current version 28 June 2024. This work was supported in part by the SiciliAn MicronanOTecH Research and Innovation Center–SAMOTHRACE (MUR, PNRR-M4C2, ECS_00000022), Spoke 3–Università Degli Studi di Palermo "S2-COMMs-Micro and Nanotechnologies for Smart and Sustainable Communities"; in part by the European Union NextGenerationEU—National Sustainable Mobility Center CN00000023 (MUR D.n. 1033—17/06/2022), Spoke 12, CUP B73C22000760001; and in part by the European Union NextGenerationEU (MUR D.M. 737/2021)—Sustainable MAterials foR novel Thin film solar cells—European Union NextGenerationEU, Italian Ministry of University and Research (EUROSMART), Bando EUROSTART (D.R. 698/2022). The review of this letter was arranged by Editor T.-Y. Seong. *(Corresponding author: Isodiana Crupi.)*

Isodiana Crupi, Roberto Macaluso, and Mauro Mosca are with the Engineering Department, University of Palermo, 90128 Palermo, Italy (e-mail: isodiana.crupi@unipa.it).

Gabriele Bellocchi, Paolo Badalà, and Simone Rascunà are with STMicroelectronics, 95121 Catania, Italy.

Roberto Vabres is with the Engineering Department, University of Palermo, 90128 Palermo, Italy, and also with STMicroelectronics, 95121 Catania, Italy.

Corrado Bongiorno is with CNR-IMM, 95121 Catania, Italy.

Color versions of one or more figures in this letter are available at https://doi.org/10.1109/LED.2024.3403797.

Digital Object Identifier 10.1109/LED.2024.3403797

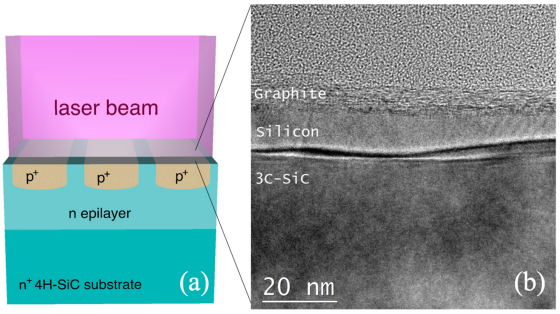

Fig. 1. Schematic illustration of SiC JBS structures under laser irradiation at the front side (a) and cross-sectional TEM image of the p^+ implanted 4H-SiC layer irradiated with four pulses at 2.4 J/cm^2 (b).

By utilizing the entire available surface, on both front and rear sides, regardless of the presence of electrical contacts, while simplifying the manufacturing process, we pave the way for a metal-free bifacial SiC based UV detector.

II. Experimental Details

Heavily nitrogen-doped 4H-SiC n^+ substrates, with resistivity of 20 mΩ·cm and thickness of 350 μm, were covered by an epitaxially grown n-type drift layer, with carrier concentration of 10^{16} cm^{-3} and thickness of 5 μm. Aluminium ion implantation was used to create anode regions, followed by thermal annealing to activate dopants and form areas with concentration of the order of 10^{19} cm^{-3} and depth of 0.6 μm. Next, the sample was exposed to pulsed excimer laser irradiation at wavelength of 310 nm and duration of 160 ns, with fluences ranging between 1 and 4 J/cm^2 and number of pulses between 1 and 5. The area of the spot of the laser beams is 1 cm^2 and, to fully cover the front surface of the device, one or more scans of the laser can be performed. Fig. 1 (a) depicts the schematic of the JBS device under PLA at the front side.

Optical transmission spectra were acquired with a Varian DMS 90 UV/Vis spectrophotometer, microstructural characteristics were investigated with a 200 kV JEOL2010F transmission electron microscopy (TEM). The electrical properties were studied using a two-terminal current–voltage (I–V) method, as well as transmission line model (TLM) structures employing Ti contacts on a Karl Suss Microtec probe station equipped with a HP 4156B parameter analyzer.

III. Results and Discussion

Fig. 1 (b) shows the cross-sectional TEM image of an anode region irradiated with four laser pulses at 2.4 J/cm^2. The formation on the surface of an ohmic-contact layer, including carbon clusters (e.g., graphite layer), is due to the thermal decomposition of the p^+ implanted 4H-SiC [20], [21], [22]. During the laser process, Si undergoes sublimation, resulting in the formation of an 8 nm graphite region, multilayer epitaxial graphene [23], and an underlying crystalline Si layer of 12 nm. At greater depths, the temperature drops to values that no longer induce the transformation of SiC into carbon-rich layers. However, due to the melting and subsequent recrystallization of the implanted 4H-SiC layer, a distinct polytype, 3C-SiC, can be observed beneath the Si layer. As a result, the laser-induced contact is limited to the surface level,

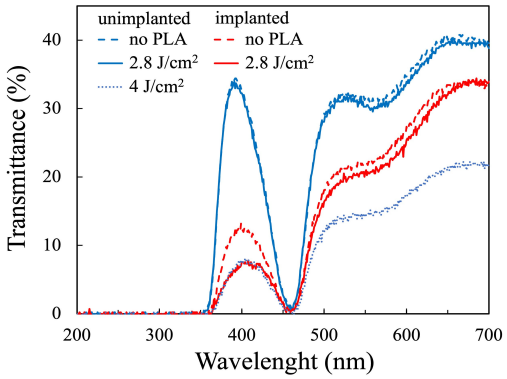

Fig. 2. Optical transmittance spectra of the n-doped unimplanted sample (blue) and the p+ implanted sample (red) before and after the annealing with two laser pulses.

it is self-aligned with the implanted region and does not extend throughout its entire thickness. Phase separation and surface graphitization are also observed in the uppermost part of n-doped unimplanted 4H-SiC but at laser fluences exceeding 3.2 J/cm^2. Due to its crystalline structure, this fluence threshold for graphitization, Φ_G, is higher than the one required for the implanted regions, where the presence of defects accelerates the mechanisms contributing to the onset of SiC graphitization. Fig. 2 shows the transmittance spectra of unimplanted and p^+ implanted 4H-SiC, before and after PLA with two laser pulses at different energy fluences. All samples exhibit a common absorption edge around 360 nm, corresponding to the transition of electrons from the valence to the conduction band [24]. Beyond this edge, the transmittance initially increases, with a peak around 400 nm, and then exhibits a decline with a value approaching to zero at 460 nm. This is related to a distinctive absorption spike at 460 nm, conventionally attributed to the transition of free electrons from the nitrogen donor level to a higher conduction band [25], [26]. It is worth noting that, compared to the unimplanted sample, the transmittance of the p^+ implanted one is lower at all measured wavelength, consistent with the higher absorption of light caused by the defect states within the bandgap, attributed to the Al implantation process. In addition, while PLA with two laser pulses at 2.8 J/cm^2 has no effects on the transmittance spectra of the unimplanted sample, it causes a reduced intensity in the 400 nm peak, with a corresponding increase in the absorption, due to the recovery of lattice damage by laser annealing. To achieve a similar peak in the unimplanted sample, a fluence of 4 J/cm^2 is required, which additionally leads to a reduction in transmittance beyond 460 nm wavelength. It should be noted that these changes in the transmittance spectra are not due to the formation of the multilayer epitaxial graphene. Indeed, according to Huang et al. [27], thanks to its unique band structure, the graphene has a wavelength-independent transmittance of about 0.977. This high optical transparency allows the underlying substrate to absorb all the incident light. The evolution of the transmittance peak intensity with the energy fluence in the blue to violet region, $T_{max\ 350-450nm}$, is reported in Fig. 3, for both implanted and unimplanted samples. While the laser energy, up to 2.8 J/cm^2, does not impact the transmittance

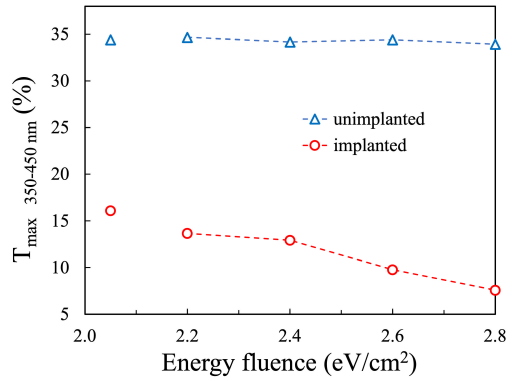

Fig. 3. Evolution of the maximum value of the optical transmittance in the 350-450 nm range as a function of the laser energy fluence for the unimplanted (blue triangles) and the implanted (red circles) 4H-SiC samples. The PLA was performed with 2 laser pulses.

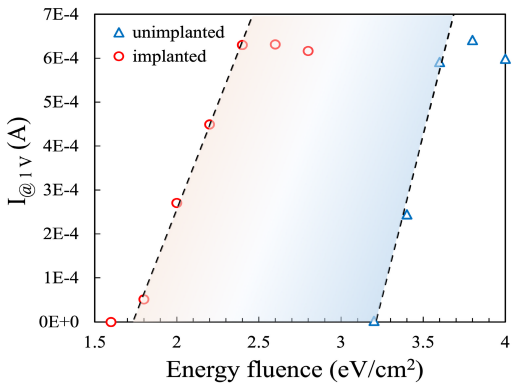

Fig. 5. Variations in current readings at 1V with increasing laser fluences for unimplanted (blue triangles) and p+ implanted (red circles) samples. The dashed lines are the linear fits, the shaded region highlights the fluence shift.

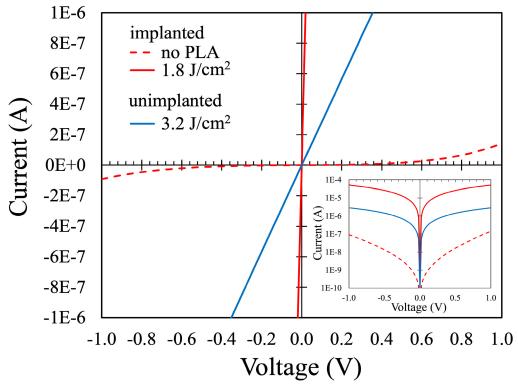

Fig. 4. I–V curves measured on unimplanted sample (blue) after two laser pulses at fluence of 3.2 J/cm^2, on p$^+$ implanted (red) not exposed to PLA and after two laser pulses at fluence of 1.8 J/cm^2. The inset shows the same data in semilogarithmic scale.

of the unimplanted sample, a gradual reduction is observed, with increasing energy fluence, in presence of implantation. It should be noted that the graphite layers, formed at these laser energies only on implanted samples, affect transmittance in the visible, without interfering with the UV region, which is essential for SiC photodetector functionality. Fig. 4 shows I-V curves before and after PLA treatment. The laser irradiation with two pulses at 1.8 J/cm^2 and 3.2 J/cm^2 promotes the formation of an upper conductive carbon region on the implanted and unimplanted 4H-SiC, respectively. This leads to a successful ohmic contact formation. On the contrary, a Schottky behavior is observed for the as-implanted sample not exposed to PLA. Ohmic behavior was achieved by placing probe heads directly on irradiated film surfaces without the use of any metal electrodes. Establishing laser-induced ohmic contacts on the unimplanted region requires a significantly higher energy density of the laser beam compared to the implanted regions. To investigate this fluence shift, samples showing a linear I-V characteristic are presented in Fig. 5. Here, the values of current at 1V, $I_{@1V}$, after two laser pulses at different fluences are compared. A rise in $I_{@1V}$ with fluence is initially observed, followed by a saturation behavior of about 60 μA in both cases. This reveals a modification in the contact composition until a stable situation is reached. The n-doped unimplanted samples require systematically higher fluences than the p$^+$ implanted ones to reach similar $I_{@1V}$. Furthermore, before the saturation region, clear linear fits between the $I_{@1V}$ and the energy fluences are found for both implanted and unimplanted 4H-SiC with approximately the same slope (0.00096 and 0.0015, respectively) but different Φ_G (1.6 J/cm^2 and 3.2 J/cm^2, respectively). This proves that the process of graphitization is the same for the two cases with an evident fluence shift due to the lower bonding energy of the p-implanted region respect to the unimplanted one. The energy needed to break the Si-C bonding is provided by the laser beam. In the implanted region, where the bonds are partially broken, the graphitization process initiates at 1.6 J/cm^2, while for the unimplanted region the same process begins at 3.2 J/cm^2. Finally, using TLM, a sheet resistance of 390 kΩ/sq and a specific contact resistance of $1.65{\cdot}10^{-2}$ Ωcm^2 was measured on sample representative of the saturation behavior in Fig 5. Respect to the conventional metallic contact, such as 100 nm Nickel formed after a rapid thermal annealing process at high temperature, our samples exhibit an increase of the specific contact resistance of about 2 orders of magnitude. This result is promising, especially when considering the differences in thickness of the ohmic contact layer, the annealing process, and optical transmittance.

IV. Conclusion

A promising approach to realize SiC based UV photodetectors with no metallic electrodes is proposed. The ohmic-contact regions on both the front and the rear can be generated by PLA with different fluences.

References

[1] E. Monroy, F. Omn S, and F. Calle, "Wide-bandgap semiconductor ultraviolet photodetectors," *Semiconductor Sci. Technol.*, vol. 18, no. 4, pp. R33–R51, Apr. 2003, doi: 10.1088/0268-1242/18/4/201.

[2] D.-S. Tsai, W.-C. Lien, D.-H. Lien, K.-M. Chen, M.-L. Tsai, D. G. Senesky, Y.-C. Yu, A. P. Pisano, and J.-H. He, "Solar-blind photodetectors for harsh electronics," *Sci. Rep.*, vol. 3, no. 1, p. 2628, Sep. 2013, doi: 10.1038/srep02628.

[3] X. Chen, H. Zhu, J. Cai, and Z. Wu, "High-performance 4H-SiC-based ultraviolet p-i-n photodetector," *J. Appl. Phys.*, vol. 102, no. 2, Jul. 2007, Art. no. 024505, doi: 10.1063/1.2747213.

[4] A. Aldalbahi, E. Li, M. Rivera, R. Velazquez, T. Altalhi, X. Peng, and P. X. Feng, "A new approach for fabrications of SiC based photodetectors," *Sci. Rep.*, vol. 6, no. 1, p. 23457, Mar. 2016, doi: 10.1038/srep23457.

[5] F. La Via, A. Severino, R. Anzalone, C. Bongiorno, G. Litrico, M. Mauceri, M. Schoeler, P. Schuh, and P. Wellmann, "From thin film to bulk 3C-SiC growth: Understanding the mechanism of defects reduction," *Mater. Sci. Semicond. Process.*, vol. 78, pp. 57–68, May 2018, doi: 10.1016/j.mssp.2017.12.012.

[6] E. M. Huseynov and T. G. Naghiyev, "Study of thermal parameters of nanocrystalline silicon carbide (3C-SiC) using DSC spectroscopy," *Appl. Phys. A, Solids Surf.*, vol. 127, no. 4, p. 267, Apr. 2021, doi: 10.1007/s00339-021-04410-2.

[7] A. Boughelout, R. Macaluso, I. Crupi, B. Megna, A. Brighet, M. Trari, and M. Kechouane, "Effect of the Si doping on the properties of AZO/SiC/Si heterojunctions grown by low temperature pulsed laser deposition," *Semicond. Sci. Technol.*, vol. 36, no. 1, Jan. 2021, Art. no. 015001, doi: 10.1088/1361-6641/abbc42.

[8] F. Nava, G. Bertuccio, A. Cavallini, and E. Vittone, "Silicon carbide and its use as a radiation detector material," *Meas. Sci. Technol.*, vol. 19, no. 10, Oct. 2008, Art. no. 102001, doi: 10.1088/0957-0233/19/10/102001.

[9] J. Fan and P. K. Chu, "General properties of bulk SiC," in *Silicon Carbide Nanostructures* (Engineering Materials and Processes). Cham, Switzerland: Springer, 2014, pp. 7–114, doi: 10.1007/978-3-319-08726-9_2.

[10] L. C. Yu, G. T. Dunne, K. S. Matocha, K. P. Cheung, J. S. Suehle, and K. Sheng, "Reliability issues of SiC MOSFETs: A technology for high-temperature environments," *IEEE Trans. Device Mater. Rel.*, vol. 10, no. 4, pp. 418–426, Dec. 2010, doi: 10.1109/TDMR.2010.2077295.

[11] J. F. Seely, B. Kjornrattanawanich, G. E. Holland, and R. Korde, "Response of a SiC photodiode to extreme ultraviolet through visible radiation," *Opt. Lett.*, vol. 30, no. 23, p. 3120, Dec. 2005, doi: 10.1364/OL.30.003120.

[12] F. Roccaforte, P. Fiorenza, G. Greco, R. Lo Nigro, F. Giannazzo, F. Iucolano, and M. Saggio, "Emerging trends in wide band gap semiconductors (SiC and GaN) technology for power devices," *Microelectron. Eng.*, vols. 187–188, pp. 66–77, Feb. 2018, doi: 10.1016/j.mee.2017.11.021.

[13] L. M. Porter and R. F. Davis, "A critical review of ohmic and rectifying contacts for silicon carbide," *Mater. Sci. Eng., B*, vol. 34, nos. 2–3, pp. 83–105, Nov. 1995, doi: 10.1016/0921-5107(95)01276-1.

[14] F. Roccaforte, F. La Via, and V. Raineri, "Ohmic contacts to SIC," *Int. J. High Speed Electron. Syst.*, vol. 15, no. 4, pp. 781–820, Dec. 2005, doi: 10.1142/s0129156405003429.

[15] S. Rascunà, P. Badalà, C. Tringali, C. Bongiorno, E. Smecca, A. Alberti, S. Di Franco, F. Giannazzo, G. Greco, F. Roccaforte, and M. Saggio, "Morphological and electrical properties of nickel based ohmic contacts formed by laser annealing process on n-type 4H-SiC," *Mater. Sci. Semicond. Process.*, vol. 97, pp. 62–66, Jul. 2019, doi: 10.1016/j.mssp.2019.02.031.

[16] C. Berger, D. Alquier, and J. F. Michaud, "Optimisation of ti ohmic contacts formed by laser annealing on 4H-SiC," *Mater. Sci. Forum*, vol. 1062, pp. 219–223, May 2022, doi: 10.4028/p-6z36aj.

[17] G. Bellocchi, R. Vabres, M. Vivona, P. Badalà, V. Puglisi, P. Mancuso, F. Giannazzo, I. Crupi, F. Roccaforte, and S. Rascuna, "Formation of Ti ohmic contact on p-SiC by laser annealing," presented at the Int. Conf. Silicon Carbide Related Mater. (ICSCRM), Sorrento, Italy, Sep. 2023.

[18] F. La Via, F. Roccaforte, A. Makhtari, V. Raineri, P. Musumeci, and L. Calcagno, "Structural and electrical characterisation of titanium and nickel silicide contacts on silicon carbide," *Microelectron. Eng.*, vol. 60, nos. 1–2, pp. 269–282, Jan. 2002, doi: 10.1016/s0167-9317(01)00604-9.

[19] S. Rascuná, G. Bellocchi, P. Badalà, and I. Crupi, "Method for manufacturing a UV-radiation detector device based on SiC, and UV-radiation detector device based on SiC," U.S. Patent 11 605 751 B2, Mar. 14, 2023.

[20] I. Choi, H. Y. Jeong, H. Shin, G. Kang, M. Byun, H. Kim, A. M. Chitu, J. S. Im, R. S. Ruoff, S.-Y. Choi, and K. J. Lee, "Laser-induced phase separation of silicon carbide," *Nature Commun.*, vol. 7, no. 1, p. 13562, Nov. 2016, doi: 10.1038/ncomms13562.

[21] M. G. Lemaitre, S. Tongay, X. Wang, D. K. Venkatachalam, J. Fridmann, B. P. Gila, A. F. Hebard, F. Ren, R. G. Elliman, and B. R. Appleton, "Low-temperature, site selective graphitization of SiC via ion implantation and pulsed laser annealing," *Appl. Phys. Lett.*, vol. 100, no. 19, May 2012, Art. no. 193105, doi: 10.1063/1.4707383.

[22] M. Vivona, F. Giannazzo, G. Bellocchi, S. E. Panasci, S. Agnello, P. Badalà, A. Bassi, C. Bongiorno, S. Di Franco, S. Rascunà, and F. Roccaforte, "Effects of excimer laser irradiation on the morphological, structural, and electrical properties of aluminum-implanted silicon carbide (4H-SiC)," *ACS Appl. Electron. Mater.*, vol. 4, no. 9, pp. 4514–4520, Sep. 2022, doi: 10.1021/acsaelm.2c00748.

[23] W. Norimatsu and M. Kusunoki, "Growth of graphene from SiC0001 surfaces and its mechanisms," *Semicond. Sci. Technol.*, vol. 29, no. 6, Jun. 2014, Art. no. 064009, doi: 10.1088/0268-1242/29/6/064009.

[24] X. Liu, S.-Y. Zhuo, P. Gao, W. Huang, C.-F. Yan, and E.-W. Shi, "Donor-acceptor-pair emission in fluorescent 4H-SiC grown by PVT method," *AIP Adv.*, vol. 5, no. 4, Apr. 2015, Art. no. 047133, doi: 10.1063/1.4919012.

[25] R. Weingärtner, M. Bickermann, S. Bushevoy, D. Hofmann, M. Rasp, T. L. Straubinger, P. J. Wellmann, and A. Winnacker, "Absorption mapping of doping level distribution in n-type and p-type 4H-SiC and 6H-SiC," *Mater. Sci. Eng., B*, vol. 80, nos. 1–3, pp. 357–361, Mar. 2001, doi: 10.1016/s0921-5107(00)00599-7.

[26] I. P. Vali, P. K. Shetty, M. G. Mahesha, V. G. Sathe, D. M. Phase, and R. J. Choudhary, "Structural and optical studies of gamma irradiated N-doped 4H-SiC," *Nucl. Instrum. Methods Phys. Res. B, Beam Interact. Mater. At.*, vol. 440, pp. 101–106, Feb. 2019, doi: 10.1016/j.nimb.2018.12.016.

[27] K. Huang, X. Yu, J. Cong, and D. Yang, "Progress of graphene–silicon heterojunction photovoltaic devices," *Adv. Mater. Interfaces*, vol. 5, no. 24, Dec. 2018, Art. no. 1801520, doi: 10.1002/admi.201801520.

Open Access funding provided by 'Università degli Studi di Palermo' within the CRUI CARE Agreement